



ORIGINAL ARTICLE

Comparison of Gd-Bz-TTDA, Gd-EOB-DTPA, and Gd-BOPTA for dynamic MR imaging of the liver in rat models

Twei-Shiun Jaw^{a,b,*}, Shih-Hsien Chen^a, Yun-Ming Wang^d, Jui-Sheng Hsu^{a,b}, Yu-Ting Kuo^{a,b}, Yen-Yu Chiu^a, Kun-Bow Tsai^c, Tsyh-Jyi Hsieh^{a,b}, Gin-Chung Liu^{a,b}

^a Department of Medical Imaging, Kaohsiung Medical University Hospital, Kaohsiung, Taiwan

^b Department of Radiology, School of Medicine, Kaohsiung Medical University, Kaohsiung, Taiwan

^c Department of Pathology, School of Medicine, Kaohsiung Medical University, Kaohsiung, Taiwan

^d Department of Biological Science and Technology, National Chiao Tung University, Hsinchu, Taiwan

Received 11 April 2011; accepted 10 June 2011

Available online 20 January 2012

KEYWORDS

Magnetic resonance imaging;
Contrast agents;
Hepatobiliary

Abstract To evaluate the competitive potential of a new lipophilic paramagnetic complex, Gd-Bz-TTDA [4-benzyl-3,6,10-tri (carboxymethyl)-3,6,10-triazado-decanedioic acid] compared with two other commercially available MR hepatobiliary contrast agents, gadobenate dimeglumine (Gd-BOPTA) and gadoxetic acid (Gd-EOB-DTPA), dynamic MR imaging studies were performed on normal and hepatocellular carcinoma (HCC) rat models using a 1.5-Tesla MR scanner. The results indicate that normal rats that were injected with 0.1 mmol/kg Gd-Bz-TTDA showed significantly more intense and persistent liver enhancement than those that were injected with the same dose of Gd-EOB-DTPA or Gd-BOPTA. All of these agents showed similar enhancement patterns in the implanted HCC. The liver-lesion contrast-to-noise ratios were higher and more persistent in rats that were injected with Gd-Bz-TTDA. These results indicate that Gd-Bz-TTDA is comparable with the commercially available hepatobiliary agents, Gd-EOB-DTPA and Gd-BOPTA, and can result in more intense and prolonged liver enhancement while still providing better liver-lesion discrimination. These results warrant further large-scale studies.
Copyright © 2012, Elsevier Taiwan LLC. All rights reserved.

Introduction

In recent years, three hepatobiliary-specific contrast agents—mangafodipir trisodium (Mn-DPDP, Teslascan, GE Healthcare, Oslo, Norway), gadobenate dimeglumine (Gd-BOPTA, MultiHance, Bracco, Milan, Italy) and gadoxetic acid (Gd-EOB-DTPA, Primovist, Bayer, Berlin, Germany)—have

* Corresponding author. Department of Medical Imaging, Kaohsiung Medical University Hospital, 100 Tz-You 1st Road, Kaohsiung, 807, Taiwan.

E-mail address: tsjaw@kmu.edu.tw (T.-S. Jaw).

been become clinically available for use in magnetic resonance imaging (MRI) [1]. The two gadolinium-based agents are able to initially distribute throughout the extracellular fluid spaces as an extracellular contrast agents and are subsequently and selectively taken up by the hepatocytes [1–3]. These contrast agents have proven their usefulness for improving lesion detection in MR imaging of the liver, as well as for characterizing the hepatocellular and non-hepatocellular properties of liver tumors [1,2,4–7].

We have developed and characterized a new lipophilic paramagnetic complex, Gd-Bz-TTDA [4-benzyl-3,6,10-tri(carboxymethyl)-3,6,10-triazado-decanedioic acid], which was designed for use as hepatic MR contrast agent [8,9]. The preliminary results of our previous study showed intense liver enhancement in normal rats lasting from 5 minutes to 3 hours. Gd-Bz-TTDA can also improve tumor conspicuity in late phase images by providing intense liver enhancement [10]. A toxicity study was also conducted that shows that it is safe for these purposes [10]. The R1 relaxivity of Gd-Bz-TTDA is superior to Gd-BOPTA. Its rotational correlation time is longer than Gd-EOB-DTPA, and its water-exchange lifetime is significantly shorter than Gd-EOB-DTPA and Gd-BOPTA [8,9]. To evaluate the competitive potential of this novel contrast agent against Gd-EOB-DTPA and Gd-BOPTA, dynamic MR imaging studies of the livers of normal rats and rats with implanted HCC were performed using these three agents.

Materials and methods

Study design

For the MR imaging studies, 12 normal male Wistar rats (National Laboratory Animal Breeding and Research Center, Taipei, Taiwan) were used, each weighing 200–250 g. Three rats were randomly assigned to each group. At each MR scan, three rats were immobilized on the same polystyrene board after being anesthetized. Each group received intravenous injection of 0.1 mmol/kg Gd-Bz-TTDA, Gd-EOB-DTPA, or Gd-BOPTA respectively. A marker was administered to each rat, and the type of contrast agent that was given was recorded. During the next study, which occurred at least 3 days later, each rat received a different contrast agent that was administered in the first study. During the third MR imaging study, which also occurred at least for 3 days later, each rat received the remaining contrast agent that they had not received in either of the two previous studies. A total of six rats with implanted HCC (Cheng hepatoma ascites [CHA], AS 30-D; Academia Sinica, Taipei, Taiwan) were also studied. MR imaging studies of the rats with HCC used a similar experimental design as that described above.

Animal models

The CHA hepatoma model [11] was successfully conducted by percutaneously injecting 0.25 mL (10^7 – 10^8 cells/mL) of the CHA suspension into six Wistar rats. A CHA hepatoma usually takes 1–3 weeks to reach its predetermined size. The experiment was performed 3 weeks after implantation, when the tumors measured at least 1 cm in diameter.

MR imaging

The rats were anesthetized with an intraperitoneal injection of sodium pentobarbital at a dose of 40–50 mg/kg. The tail veins were cannulated using a 1-mL disposable syringe filled with the contrasting agent. The rats were then placed in a head coil in the prone position. MR imaging was performed using a 1.5-T superconductive MR scanner (Gyrosan ACS-NT; Philips Medical Systems, Best, Netherlands). T1- and T2-weighted coronal spin echo (SE) images were acquired as the baseline images. Sequential T1-weighted turbo field-echo (TFE) (TR/TE/flip angle: 15 msec/6.1 msec/25°) coronal images were obtained before and after intravenous injection of the contrasting agents. The following parameters were used: number of excitations, two; field of view, 20 cm; slice thickness, 4 mm; and image matrix, 256 × 128. To assess any dynamic changes in enhancement, postcontrast scans were obtained every 14 seconds for nine continuous scans, every 5 minutes for six subsequent scans, and every 10 minutes for up to 2 hours. Similar protocols with additional T2-weighted images were used on the rats with implanted HCC, both before and after the intravenous injection one of the three contrast agents. During scanning, a glass cylinder containing 2% weight/volume agarose gel was positioned adjacent to the rats as a reference standard.

Image analysis

Operator-defined regions of interest were selected for the liver parenchyma, away from vessels or artifacts, and from the agarose gel reference standard. Approximately 0.1 cm² was used for the regions of interest in the liver and the solid and necrotic compartments of the tumors. The operator was blind to information regarding which contrast agents had been injected into the individual rats.

MR images were analyzed in order to evaluate any time-enhancement changes that occurred in the livers of the normal rats that could be identified using the three contrast agents. The signal intensity of each target was normalized by dividing its mean target-signal intensity by that of the agarose gel standard (signal-to-noise ratio, SI/N). The enhancement percentage of the liver was calculated as follows:

$$\text{Enhancement \%} = \frac{(SI/N)_t - (SI/N)_{pre}}{(SI/N)_{Dre}} \times 100\%$$

In this equation, (SI/N)_t and (SI/N)_{pre} are the post-contrast and precontrast signal-to-noise ratios of the liver, respectively. The enhancement percentages at different time points were compared for each contrast agent. Results are expressed as the mean ± SD. The Student *t* test was used to compare differences between two of the three groups. A *p*-value <0.05 was considered statistically significant. Lesion conspicuity was assessed by the percentage increase in the liver-lesion contrast-to-noise ratio (CNR) using the following formula:

% Increase of Liver-Lesion CNR

$$= \frac{[(SI_{liver} - SI_{lesion})/N]_t - [(SI_{liver} - SI_{lesion})/N]_{pre}}{[(SI_{liver} - SI_{lesion})/N]_{pre}} \times 100\%$$

The solid and necrotic compartments of the liver tumors were assessed separately as the percentage of increase in liver-lesion CNR.

Histopathological confirmation

The rats with implanted HCC were sacrificed immediately after the last MR scan by cardiac exsanguinations under deep anesthesia with ether. The livers implanted with HCC were removed and fixed in 10% formalin following autopsy. Paraffin-embedded sections and eosin-stained preparations were microscopically observed to determine the presence of HCC.

Results

The time-enhancement changes that occurred in the normal rats after being injected with 0.1 mmol/kg Gd-Bz-TTDA, Gd-EOB-DTPA or Gd-BOPTA are shown in Fig. 1. Liver enhancement in the normal rats rose rapidly during the first 5 minutes in each group. After that, liver enhancement plateaued in the Gd-Bz-TTDA group, then steadily but slowly declined over the next 2 hours. Liver enhancement in normal rats injected with Gd-EOB-DTPA or Gd-BOPTA peaked at 5 minutes after injection, then gradually declined. At 10 minutes and thereafter, Gd-Bz-TTDA produced significantly better liver enhancement than Gd-EOB-DTPA and Gd-BOPTA. (At 10 minutes, Gd-Bz-TTDA [$152.3 \pm 26.3\%$] vs. Gd-EOB-DTPA [$130.5 \pm 22.8\%$], $p < 0.05$; Gd-Bz-TTDA vs. Gd-BOPTA [$106.7 \pm 22.7\%$]; $p < 0.001$) (Fig. 1). As shown in Table 1, there are no statistical differences in the percentages of liver enhancement measured in each of the three group during the arterial, venous, or equilibrium phases. At 5 minutes, there were significantly higher percentages of liver enhancement in the Gd-Bz-TTDA and Gd-EOB-DTPA groups compared with the Gd-BOPTA group ($p < 0.05$). Gd-Bz-TTDA produced significantly more intense enhancement in liver than the other two groups at each time point after 30 minutes ($p < 0.001$) (Table 1).

The livers of the normal rats that were injected with Gd-Bz-TTDA, Gd-EOB-DTPA, or Gd-BOPTA showed similar

Table 1 The liver enhancement (%) in normal rats during various phases after injection of 0.1 mmol/kg Gd-Bz-TTDA, Gd-EOB-DTPA, or Gd-BOPTA.

Phases	Bz-TTDA	EOB-DTPA	BOPTA
Arterial (28 sec)	82.9 ± 23.4	86.2 ± 20.0	80.5 ± 15.2
Venous (70 sec)	124.8 ± 28.4	136.9 ± 28.3	111.6 ± 33.5
Equilibrium (126 sec)	138.5 ± 31.0	139.2 ± 32.7	115.7 ± 33.4
Hepatobiliary			
5 min	$151.0 \pm 40.5^*$	$150.2 \pm 32.7^*$	115.3 ± 35.8
30 min	$125.6 \pm 21.6^{**}$	78.7 ± 28.5	74.3 ± 30.6
60 min	$117.4 \pm 27.3^{**}$	48.9 ± 12.4	47.2 ± 23.1
120 min	$110.8 \pm 30.9^{**}$	17.9 ± 11.0	25.6 ± 9.5

(mean \pm standard deviation, $n = 12$ in each group).

* $p < 0.05$: Bz-TTDA vs. BOPTA at 5 minutes; EOB-DTPA vs. BOPTA at 5 minutes.

** $p < 0.001$: Bz-TTDA vs. EOB-DTPA; Bz-TTDA vs BOPTA at 30, 60, and 120 minutes.

enhancement patterns in the dynamic contrast study, demonstrating rapidly increased enhancement during the arterial phase, more intense enhancement during the venous phase, and steady enhancement during the equilibrium phase, as shown in Fig. 2. After 5 minutes, the liver parenchyma of rats injected with Gd-Bz-TTDA and Gd-EOB-DTPA showed relatively more intense enhancement than the liver parenchyma of rats injected with Gd-BOPTA. After 30 minutes, Gd-Bz-TTDA produced more intense enhancement of the liver parenchyma in normal rats than Gd-EOB-DTPA and Gd-BOPTA (Fig. 2).

Sequential MR images of a rat with implanted HCC before and after intravenous injection of 0.1 mmol/kg Gd-Bz-TTDA, Gd-EOB-DTPA, and Gd-BOPTA are shown in Fig. 3. All agents demonstrated similar enhancement patterns of the implanted HCC, with significant enhancement of the solid compartment of the tumor and no enhancement of the centrally necrotic parts. These findings are consistent with the gross pictures of the autopsy specimens and their pathohistological features (Fig. 3D, E). After 5 minutes,

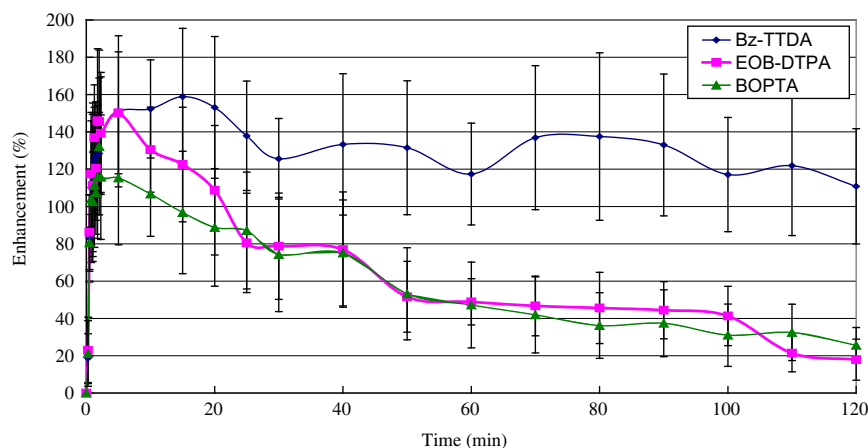


Figure 1. Time-enhancement changes in the livers of normal rats after the injection of 0.1 mmol/kg Gd-Bz-TTDA, Gd-EOB-DTPA, or Gd-BOPTA on T1-weighted images (mean \pm standard deviation, $n = 12$ in each group).

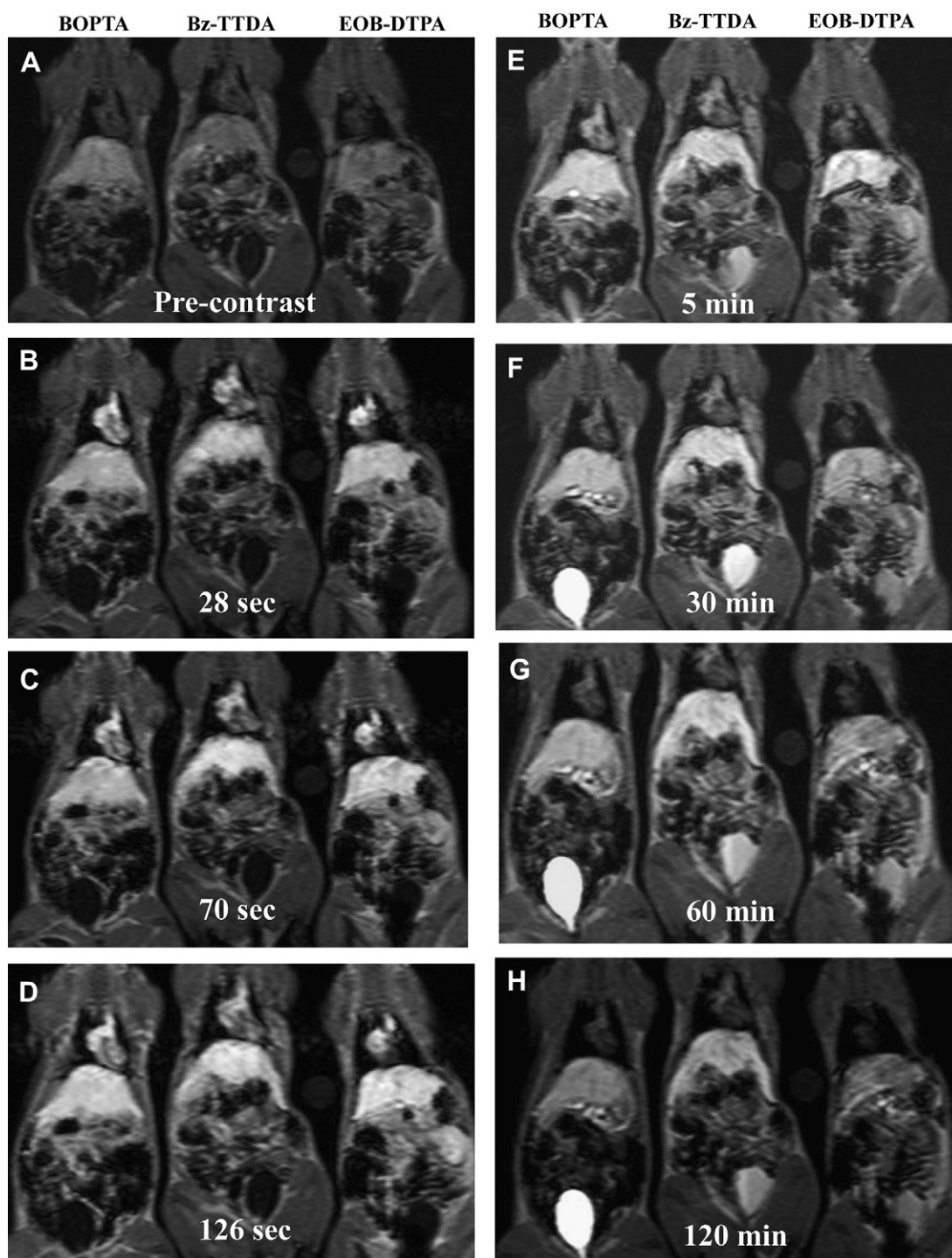


Figure 2. Gd-Bz-TTDA, Gd-EOB-DTPA, and Gd-BOPTA enhanced dynamic T1-weighted TFE images in normal rats. A: Precontrast images. B: Arterial phase at 28 seconds. C: Venous phase at 70 seconds. D: Equilibrium phase at 126 seconds. E, F, G, and H: Hepatobiliary phase at 5–120 minutes. Gd-Bz-TTDA produced more intense enhancement in liver than the other two groups at 30, 60, and 120 minutes. Circle: reference standard.

good liver-lesion discrimination was observed in all groups because tumor enhancement had gradually been washed out, but intense liver enhancement was also achieved. After 60 minutes, liver enhancement faded in rats that were injected with Gd-EOB-DTPA or Gd-BOPTA, whereas intense liver enhancement persisted and good liver-lesion

discrimination remained in rats injected with Gd-Bz-TTDA (Fig. 3).

Quantitative analyses of the percentage increase in liver-lesion CNR in rats with HCC after injection of Gd-Bz-TTDA, Gd-EOB-DTPA, or Gd-BOPTA are compared in Fig. 4. Liver-lesion CNRs were also higher in rats injected with Gd-Bz-

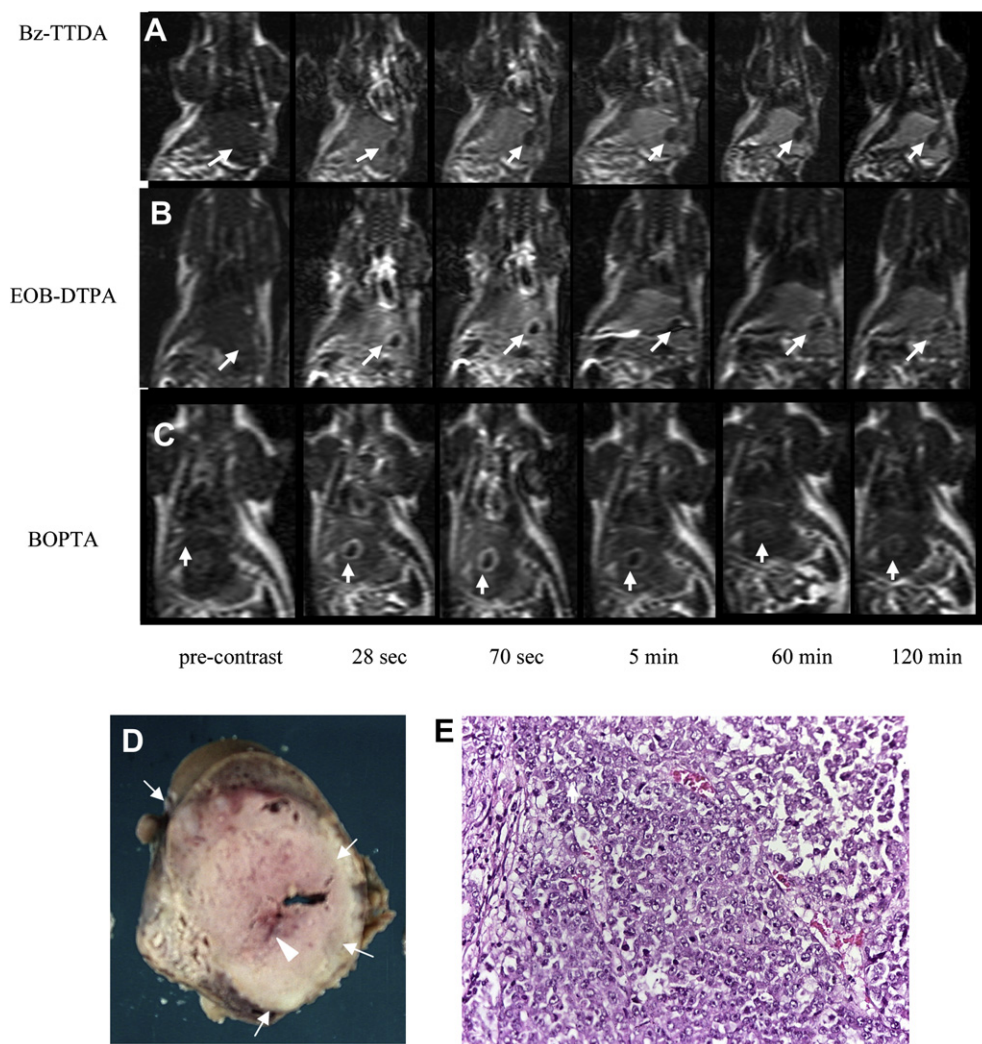


Figure 3. Sequential T1-weighted TFE images of a rat with implanted HCC before and after injection of 0.1 mmol/kg Gd-Bz-TTDA (A), Gd-EOB-DTPA (B), or Gd-BOPTA (C). In the images recorded at 28 and 70 seconds, similar degrees of tumor enhancement are noted in each group. At 5 minutes, good liver-to-lesion differentiation is demonstrated in all three groups due to the intense liver enhancement and wash-out of the tumor contrast agent. At 60 and 120 minutes, persistent and intense liver enhancement with better liver-lesion contrast is noted following the injection of Gd-Bz-TTDA; however, only faint enhancement of the liver and noticeably less discrimination of the lesions are noted in the other two groups. The arrows indicate the tumor. (D) Cut surface of an autopsied specimen with liver HCC showing central necrosis (arrow head). (E) Histological specimen demonstrating poorly differentiated HCC, which consists of dark and light cells. Mitotic features and hypervascularity are also noted. (hematoxylin and eosin stain, original magnification 80 \times).

TTDA than those injected with Gd-EOB-DTPA or Gd-BOPTA after 30 minutes.

Discussion

Gd-based hepatobiliary MR contrast agents provide the dual benefits of dynamic contrast enhancement and delayed hepatobiliary phase imaging [1,2]. During dynamic MR imaging, after the bolus injection, these agents also act as extracellular contrast agents (for example: gadopentate dimeglumine [Gd-DTPA]) for the noninvasive detection and characterization of liver tumors. Unlike extracellular contrast agents, however, which rapidly leave the vascular space and reach equilibrium with the extracellular space,

providing little benefit over unenhanced images during the equilibrium phase, hepatobiliary agents selectively accumulate in the hepatocytes, leading to an increase in contrast between the normal liver parenchyma and the lesion [12–14]. Hepatobiliary agents are also taken up by mass lesions with hepatocellular functions, such as regenerative/dysplastic nodules, focal nodular hyperplasia, and hepatic adenoma, thus contributing to the differential diagnosis of hepatic tumors [1,15]. Many reports have also indicated that contrast enhancement that is induced by the administration of hepatobiliary agents provides information on the degree of cellular differentiation in HCC [16,17].

In this study, the liver enhancement observed in the normal rats demonstrated similar enhancement patterns during the arterial, venous, and equilibrium phases of the

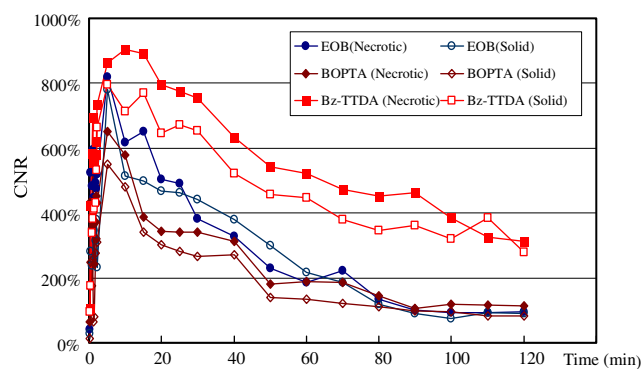


Figure 4. Percentage increase in liver-lesion CNR in rats with HCC after injection of Gd-Bz-TTDA, Gd-EOB-DTPA, or Gd-BOPTA (mean; $n = 6$ in each group; solid: solid part of tumor; necrotic: central necrotic part of the tumor).

dynamic contrast study to the two commercialized hepatobiliary contrast agents (Gd-EOB-DTPA and Gd-BOPTA). Liver enhancement increased rapidly during the first 5 minutes and then reached a plateau, which slowly decreased to 110% of enhancement at 2 hour after injection; liver enhancement of rats injected with Gd-EOB-DTPA or Gd-BOPTA peaked at 5 minutes and then steadily decreased. Significantly better liver enhancement following the administration of Gd-Bz-TTDA, in comparison with Gd-EOB-DTPA and Gd-BOPTA, was found between 10 minutes to 2 hours after injection. After 60 minutes, liver enhancement due to these the two commercial agents was below 50% while that of Gd-Bz-TTDA still remained above 110%. Our previous report showed that at 3 hours after injection of Gd-Bz-TTDA, approximately 95% of enhancement was preserved, which gradually declined to 15% at 24 hours [10]. This prolonged liver enhancement, which was still apparent up to 24 hours after injection, might be of little clinical benefit even though our preliminary subacute toxicity study in rats showed no evidence of changes to the liver [10].

The physicochemical characterization of Gd-Bz-TTDA indicated a lipophilic character and weak binding to human serum albumin, similar to Gd-EOB-DTPA [8,9]. Because of its lipophilic character and its chemical similarities to Gd-EOB-DTPA, the mechanism that allows its uptake into the liver and the biliary excretion of Gd-Bz-TTDA may also depend on an organic anion transporter (the same transport protein as bilirubin) that acts in the hepatocytes [18]. Previous reports have suggested that Gd-BOPTA is transported into rat hepatocytes via the same pathway [19]. In a rat study, the hepatic uptake transporter of Gd-EOB-DTPA was confirmed to be organic transporting polypeptide (OTAP) 1 [20] and the export transporter was confirmed as multidrug-resistant protein (MRP) 2 [21]. Recently, Kitao et al. found that enhancement of HCC in the hepatobiliary phase of Gd-EOB-DTPA is positively correlated with expression levels of OATP8 and MRP3 [7]. Tsuboyama et al. also confirmed that high hepatocyte-selective enhancement is induced by the expression patterns of these transporters, which may result in the accumulation of Gd-EOB-DTPA in the cytoplasm of HCC cells or in the lumina of pseudoglands [22]. Because there are

similarities in their chemical structures, lipophilic characters, and albumin-binding characteristics of Gd-Bz-TTDA and Gd-EOB-DTPA, the uptake and accumulation of Gd-Bz-TTDA in HCC might also involve the above mentioned transporters. Therefore, Gd-Bz-TTDA might play a role in hepatocyte-specific tumor imaging. Further investigations into the mechanisms and kinetics of Gd-Bz-TTDA in HCC tumor cells are also required.

The better and more prolonged liver enhancement that resulted from Gd-Bz-TTDA could be related to its higher relaxivity and/or hepatic uptake compared with the other two agents that were studied. The R1 relaxivity ($4.9 \text{ mM}^{-1}\text{s}^{-1}$) of Gd-Bz-TTDA is superior to Gd-BOPTA ($4.39 \text{ mM}^{-1}\text{s}^{-1}$), but slightly lower than that of Gd-EOB-DTPA ($5.3 \text{ mM}^{-1}\text{s}^{-1}$) [9,23–25]. The longer rotational correlation time and faster water-exchange lifetime also contribute to the high R1 relaxivity of Gd-Bz-TTDA [9]. The weak binding of Gd-Bz-TTDA with serum albumin may also contribute to its plasma T1 shortening, similar to Gd-EOB-DTPA and Gd-BOPTA [9,24–26]. The hepatobiliary excretion of Gd-Bz-TTDA is 75.3% in rats, according to the unpublished data of our bio-distribution study conducted using ^{111}In . This is higher than the values reported for Gd-EOB-DTPA (53.1–70%) and Gd-BOPTA (38.6–50%) [25–27].

The prolonged plateau-like enhancement of Gd-Bz-TTDA might have important practical implications because the wide postcontrast imaging window provides flexibility for managing patient workflow. Nevertheless, liver enhancement is species specific [26–29]. In rats, up to 50% of the Gd-BOPTA that is injected is excreted into the bile [26,27]. In contrast, in humans only 2–7% of Gd-BOPTA is excreted into the bile [26,28]. Up to 70% of Gd-EOB-DTPA is excreted into the bile in rats and up to 50% is excreted into the bile in humans [1,29]. Liver enhancement and biliary excretion of Gd-Bz-TTDA in humans require further evaluation. Liver enhancement of Gd-based hepatobiliary contrast agents is dose-related [25]. The clinical recommended dose of Gd-EOB-DTPA is 0.025 mmol/kg and that of Gd-BOPTA is 0.1 mmol/kg. Therefore, the results of the liver enhancement studies in this rat model cannot be directly applied to clinical situations. Further clinical trials are required.

In the MR imaging study of rats with implanted HCC, all three hepatobiliary agents demonstrated dynamic enhancement capabilities for hepatic tumors, similar to the extracellular agents. Liver-lesion discrimination was significantly enhanced during the hepatobiliary phase for all three agents. Nevertheless, the liver-lesion CNRs were higher in rats injected with Gd-Bz-TTDA than the other two groups due to more intense and prolonged liver enhancement. A previous toxicity study on Gd-Bz-TTDA revealed no changes in liver or kidney tissues when the animals were sacrificed at 14 days postinjection [10]. The LD50 (Lethal Dose, 50%) of Gd-Bz-TTDA in mice is 7.5 mmol/kg [10]. This value is comparable with the LD50 of Gd-EOB-DTPA, which ranges from 7.5–10 mmol/kg, and that of Gd-BOPTA, which ranges from 5.7–7.9 mmol/kg [25,29,30]. Toxicity studies on Gd-BOPTA and Gd-EOB-DTPA performed on animals have shown good neural and cardiovascular tolerabilities for these lipophilic contrast agents [25,31]. Nevertheless, cardiovascular and neurological adverse reactions could still occur in a clinical setting. [32,33]. The prolonged retention of Gd-Bz-TTDA in the body might raise concerns

about the increased risk of the side effects that are induced by Gd-chelated contrast agents, such as nephrogenic systemic fibrosis or cardiovascular or neural adverse reactions [32–34]. Therefore, further safety and pharmacology studies on Gd-Bz-TTDA will be required.

In conclusion, the results of this study indicate that Gd-Bz-TTDA is comparable with the commercially available hepatobiliary MR contrast agents, Gd-BOPTA and Gd-EOB-DTPA, but is characterized by more intense and prolonged liver enhancement and better liver-lesion discrimination. Therefore, further large-scale studies are warranted.

Acknowledgments

We are grateful to the National Science Council of Taiwan ROC for their financial support (NSC 93-2314-B-037-068).

References

- [1] Seale MK, Catalano OA, Saini S, Hahn PF, Vahani DV. Hepatobiliary-specific MR contrast agents: role in imaging the liver and biliary tree. *Radiographics* 2009;29:1725–48.
- [2] Semlka RC, Helmberger TK. Contrast agents for MR imaging of the liver. *Radiology* 2001;218:27–38.
- [3] Kühn JP, Hegenscheid K, Seigmund W, Froehlich CP, Hosten N, Puls R. Normal dynamic MRI enhancement patterns of the upper abdominal organs: gadoxetic acid compared with gadobutrol. *AJR Am J Roentgenol* 2009;193:1318–23.
- [4] Ba-Ssalamah A, Uffmann M, Saini S, Bastati N, Herold C, Schima W. Clinical value of MRI liver-specific contrast agents: a tailored examination for a confident non-invasive diagnosis of focal liver lesions. *Eur Radiol* 2009;19:342–57.
- [5] Ahn SS, Kim MJ, Js Lim, Hong HS, Chung YE, Choi JY. Added value of gadoxetic acid-enhanced hepatobiliary phase MR imaging in the diagnosis of hepatocellular carcinoma. *Radiology* 2010;255:459–66.
- [6] Hwang HS, Kim SH, Jeon TY, Choi DC, Lee WJ, Lim KH. Hypointense hepatic lesions depicted on gadobenate dimeglumine three-hour delayed hepatobiliary-phase MR imaging: differentiation between benignancy and malignancy. *Korea J Radiol* 2009;10:294–302.
- [7] Kitao A, Zen Y, Matsui O, Gabata T, Kobayashi S, Koda W, et al. Hepatocellular carcinoma: Signal intensity at gadoxetic acid-enhanced MR imaging; correlation with molecular transports and histopathologic features. *Radiology* 2010;256:817–26.
- [8] Wang YM, Lee CH, Liu GC, Sheu RS. Synthesis and complexation of Gd^{3+} , Ca^{2+} , Cu^{2+} , and Zn^{2+} by 3,6, 10-tri(carboxymethyl)-3,6,10-triazadodeanedioic acid. *J Chem Soc Dalton Trans*; 1998: 4113–8.
- [9] Cheng TH, Lee TM, Ou MH, Li CR, Liu GC, Wang YM. Thermodynamic stability and physicochemical characterization of ligand (4S)-4-benzyl-3,6-10-tris(carboxymethyl)-3,6,10-triazadodecanedioic acid (H5-[(s)-4-Bz-TTDA]) and its complexes formed with lanthanides, calcium (II), zinc(II), and copper (II) ions. *Helv Chim Acta* 2002;85:1033–50.
- [10] Hsu FS, Jaw TS, Liu GC, Wang YM, Chen SH, Kuo YT, et al. Evaluation of $[Gd(Bz-TTDA)]^{2-}$ as a potential contrast agent in MR imaging of the hepatobiliary system: an animal study. *J Magn Reson Imaging* 2004;20:632–9.
- [11] Smith DF, Walborg Jr EF, Chang JP. Establishment of a transplantable ascites variant of a rat hepatoma induced by 3'-methyl-4-dimethylaminoazobenene. *Cancer Res* 1970;30: 2306–9.
- [12] Caudana R, Morana G, Pirovan GP, Nicoli N, Portuese A, Spinazzi A, et al. Focal malignant hepatic lesions: MR imaging enhanced with gadolinium benzyloxypropionic tetra-acetate (BOPTA); preliminary results of phase II clinical application. *Radiology* 1996;199:513–20.
- [13] Torres CG, Lundy B, Sterud AT, McGill S, Gordo PB, Bjerknes HS. Mn-DPDP for MR imaging of the liver: results from the European phase III studies. *Acad Radiol* 1997;38:631–7.
- [14] Vogl TJ, Kummel S, Hammerstingl R, Schellenbeck M, Schumacher G, Balzer T, et al. Liver tumors: comparison of MR imaging with Gd-EOB-DTPA and Gd-DTPA. *Radiology* 1996;200: 59–67.
- [15] Grazioli L, Morana G, Federle MP, Brancatelli G, Testoni M, Kirchin MA, et al. Focal nodular hyperplasia: Morphologic and functional information from MR imaging with gadobenate dimeglumine. *Radiology* 2001;221:731–9.
- [16] Ni Y, Marchal G, Yu J, Mühler A, Lukito G, Baert AL. Prolonged positive contrast enhancement with Gd-EDB-DTPA in experimental liver tumors: potential value in tissue characterization. *J Magn Reson Imaging* 1994;4:353–63.
- [17] Manfredi R, Maresca G, Baron RL, Cotroneo AR, De Gaetano AM, De Franco A, et al. Delayed MR imaging of hepatocellular carcinoma enhanced by gadobenate dimeglumine (Gd-BOPTA). *J Magn Reson Imaging* 1999;9:704–10.
- [18] Ni Y, Marchal G, Lukito G, Yu J, Mühler A, Baert AL. MR imaging evaluation of liver enhancement by Gd-EOB-DTPA in selective and total bile duct obstruction in rats: correlation with serologic, microcholangiographic, and histologic findings. *Radiology* 1994;190:753–8.
- [19] Planchang C, Gex-Fabry M, Dornier C, Quadri R, Resit M, Invancevic K, et al. Gd-BOPTA transport into rat hepatocytes: pharmacokinetic analysis of dynamic magnetic resonance images using a hollow-fiber bioreactor. *Invest Radiol* 2004;39: 506–16.
- [20] Van Montfort JE, Stieger B, Meijer DK, Weinmann HJ, Meier PJ, Fattinger KE. Hepatic uptake of magnetic resonance imaging contrast agent gadoxetate by the organic transporting polypeptide Oatp 1. *J Pharmacol Ther* 1999;290(1):153–7.
- [21] Tsuboyana T, Onishi H, Kim T, Akita H, Hori M, Tatsumi M, et al. Hepatocellular carcinoma: hepatocyte-selective enhancement at gadoxetic acid-enhanced MR imaging—correlation with expression of sinusoidal and canalicular transporters and bile accumulation. *Radiology* 2010;255:824–33.
- [22] Lorusso V, Pascolo L, Ferneti C, Visigalli M, Anelli P, Tiribelli V. In vitro and in vivo hepatic transport of the magnetic resonance imaging contrast agent B22956/1: Role of MRP proteins. *Biochem Biophys Res Commun* 2002;293: 100–5.
- [23] Uggeri F, Aime S, Anelli PL, Botta M, Brochetia M, Haen C, et al. Novel contrast agents for magnetic resonance imaging synthesis and characterization of the ligand BOPTA and its Ln(III) complexes (Ln = Gd, Ld, Lu). X-ray structure of disodium (TPS-9-145337286-C-5)-[4-carboxyl-5,8,11-tris (carboxymethyl)-1-phenyl-2-oxa- 5,8,11-triazatridecan-13-oato(5-) gadolinite(2-) in a mixture with its enantiomer. *Inorg Chem* 1995;34:633–42.
- [24] Pintaske J, Martirosian P, Gra SH, Erb G, Lodeman KP, Claussen CD, et al. Relaxivity of gadopentetate dimeglumine (Magnevist), gadobutrol (Gadovist) and gadobenate dimeglumine (MultiHance) in human blood plasma at 0.2, 1.5 and 5 Tesla. *Invest Radiol* 2006;41:213–21.
- [25] Schuhmann-Giampierri G, Schmitt-Willich H, Press WR, Negishi C, Weinmann H-J, Speck U. Preclinical evaluation of Gd-EOB-DTPA as a contrast agent in MR imaging of the hepatobiliary system. *Radiology* 1992;183:59–64.
- [26] Lorusso V, Tiziano A, Trione P, de Haën C. Pharmacokinetics and tissue distribution in animals of gadobenate ion, the magnetic resonance imaging contrast enhancing component of gadobenate dimeglumine 0.5 M solution for injection (MultiHance). *J Comput Assist Tomogr* 1999;23:S181–94.

- [27] De Haën C, Lorusso V, Tirone P. Hepatic transport of gadobenate dimeglumine in TR rats. *Acad Radiol* 1996;3:452–4.
- [28] Spinazzi A, Lorusso V, Pirovano G, Taroni P, Kirchin M, Davies A. MultiHance clinical pharmacology. *Acad Radiol* 1998;5(Suppl.):86–9.
- [29] Weinmann HJ, Schuhmann-Giampiepi G, Schmitt-Willich H, Vogler H, Frenzel Gries H. A new lipophilic gadolinium chelate as a tissue-specific contrast medium for MRI. *Magn Reson Med* 1991;22:233–7.
- [30] Morisetti A, Bussi S, Tirone P, de Haenn C. Toxicological safety evaluation of gadobenate dimeglumine 0.5 M solution for injection (MultiHance): a new magnetic resonance imaging contrast medium. *J Comput Assist Tomogr* 1999;23: S207–17.
- [31] Tirone P, Castano M, Cipolla P, Frigeni V, Noce AL, Luzzani F, et al. General pharmacology in experimental animals of gadobenate dimeglumine (MultiHance): a new magnetic resonance imaging contrast agent. *J Comput Assist Tomogr* 1999;23:S195–206.
- [32] Abujudeh HH, Kosaraju VK, Kaewlai R. Acute adverse reactions to gadopentetate dimeglumine and gadobenate dimeglumine: experience with 32,659 injections. *AJR* 2010;194:430–4.
- [33] Bluemke DA, Sahani D, Amendola M, Balzer T, Breuer J, Brown JT, et al. Efficacy and safety of MR imaging with liver-specific contrast agent: US multicenter phase III study. *Radiology* 2005;237:89–98.
- [34] Abu-Alfa AK. Nephrogenic systemic fibrosis and gadolinium-based contrast agent. *Adv Chronic Kidney Dis* 2011;18:188–98.